

Probing extra dimensions through the invisible Higgs decay

D. DOMINICI

Dipartimento di Fisica, Università di Firenze, I-50019 Sesto F., Italy
I.N.F.N., Sezione di Firenze, I-50019 Sesto F., Italy

Received xxx;
final version xxx

In the large extra dimension model of Arkani-Hamed, Dimopoulos and Dvali the presence of an interaction between the Ricci scalar curvature and the Higgs doublet of the Standard Model makes a light Higgs boson observable at LHC at the 5σ level through the fusion process $pp \rightarrow W^*W^* + X \rightarrow \text{Higgs, graviscalars} + X \rightarrow \text{invisible} + X$ for the portion of the Higgs-graviscalar mixing (ξ) and effective Planck mass (M_D) parameter space where channels relying on visible Higgs decays fail to achieve a 5σ signal. However even if the LHC has a good chance of seeing a signal, it will not be able to determine the parameters of the model with any real precision. This goal can be reached by adding the following LC measurements: $\gamma + \cancel{E}_T$, Higgs production and decay in the visible SM-like final states and in the invisible final state.

PACS: 12.60.-i Models beyond the standard model

Key words: Extra dimensions, Invisible Higgs

1 Introduction

The effect of the invisible decay of the Higgs on the Higgs phenomenology at LHC has been recently considered. In several modifications of the Standard Model such a decay appears: as invisible decay to neutralinos in supersymmetric models (for a recent analysis see [1, 2]), as decay to Majorons [2, 3] in models with spontaneously broken lepton number or as a decay to neutrinos in fourth generation models [4]. The recent suggestion of a low scale quantum gravity (ADD) [5, 6] has added a new mechanism for predicting invisible Higgs decay, as decay to Kaluza Klein neutrino excitations [2] or to graviscalars [7–10]. In ADD models the presence of an interaction between the Higgs H and the Ricci scalar curvature of the induced 4-dimensional metric g_{ind} , given by the following action

$$S = -\xi \int d^4x \sqrt{g_{ind}} R(g_{ind}) H^\dagger H, \quad (1)$$

generates, after the usual shift $H = (\frac{v+h}{\sqrt{2}}, 0)$, the following mixing term [7]

$$\mathcal{L}_{\text{mix}} = \epsilon h \sum_{\vec{n} > 0} s_{\vec{n}} \quad (2)$$

with

$$\epsilon = -\frac{2\sqrt{2}}{M_P} \xi v m_h^2 \sqrt{\frac{3(\delta-1)}{\delta+2}}. \quad (3)$$

Above, $M_P = (8\pi G_N)^{-1/2}$ is the Planck mass, δ is the number of extra dimensions, ξ is a dimensionless parameter and $s_{\vec{n}}$ is a graviscalar KK excitation with mass $m_{\vec{n}} = 2\pi|\vec{n}|/L$, L being the size of each of the extra dimensions. After diagonalization of the full mass-squared matrix one finds that the physical eigenstate, h' , acquires admixtures of the graviscalar states and vice versa. Dropping $\mathcal{O}(\epsilon^2)$ terms and higher [10],

$$h' \sim \left[h - \sum_{\vec{m} > 0} \frac{\epsilon}{m_h^2 - im_h\Gamma_h - m_{\vec{m}}^2} s_{\vec{m}} \right], \quad s'_{\vec{m}} \sim \left[s_{\vec{m}} + \frac{\epsilon}{m_h^2 - im_h\Gamma_h - m_{\vec{m}}^2} h \right], \quad (4)$$

where Γ_h is the visible width. In computing a process such as $WW \rightarrow h' + \sum_{\vec{m} > 0} s'_{\vec{m}} \rightarrow F$, normalization and mixing corrections of order ϵ^2 that are present must be taken into account and the full coherent sum over physical states must be performed. The result at the amplitude level is [10]

$$\mathcal{A}(WW \rightarrow F)(p^2) \sim \frac{g_{WW} g_{hF}}{p^2 - m_h^2 + im_h\Gamma_h + iG(p^2) + F(p^2)}, \quad (5)$$

where $F(p^2) \equiv -\epsilon^2 \text{Re} \left[\sum_{\vec{m} > 0} \frac{1}{p^2 - m_{\vec{m}}^2} \right]$ and $G(p^2) \equiv -\epsilon^2 \text{Im} \left[\sum_{\vec{m} > 0} \frac{1}{p^2 - m_{\vec{m}}^2} \right]$. Taking the amplitude squared and integrating over dp^2 in the narrow width approximation gives the result

$$\begin{aligned} \sigma(WW \rightarrow h' + \sum_{\vec{m} > 0} s'_{\vec{m}} \rightarrow F) &= \sigma_{SM}(WW \rightarrow h \rightarrow F) \left[\frac{1}{1 + F'(m_{h\,ren}^2)} \right]^2 \\ &\times \left[\frac{\Gamma_h}{\Gamma_h + \Gamma_{h \rightarrow gravisc.}} \right], \end{aligned} \quad (6)$$

where $m_{h\,ren}^2 - m_h^2 + F(m_{h\,ren}^2) = 0$ and we have defined $m_h\Gamma_{h \rightarrow gravisc.} \equiv G(m_{h\,ren}^2)$. For a light Higgs boson both the wave function renormalization and the mass renormalization effects are small [10]. Therefore the coherently summed amplitude gives the following result for the cross section:

$$\begin{aligned} \sigma(WW \rightarrow h' + \sum_{\vec{m} > 0} s'_{\vec{m}} \rightarrow F) &\sim \sigma_{SM}(WW \rightarrow h \rightarrow F) \\ &\times \left[\frac{\Gamma_h}{\Gamma_h + \Gamma_{h \rightarrow gravisc.}} \right], \end{aligned} \quad (7)$$

where the invisible width is given by [7, 8, 10]

$$\begin{aligned} \Gamma_{h \rightarrow gravisc.} &\equiv \Gamma(h \rightarrow \sum_{\vec{n}} s_{\vec{n}}) = 2\pi\xi^2 v^2 \frac{3(\delta-1)}{\delta+2} \frac{m_h^{1+\delta}}{M_D^{2+\delta}} S_{\delta-1} \\ &\sim (16\,MeV) 20^{\delta-2} \xi^2 S_{\delta-1} \frac{3(\delta-1)}{\delta+2} \left(\frac{m_h}{150\,GeV} \right)^{1+\delta} \left(\frac{3\,TeV}{M_D} \right)^{2+\delta}, \end{aligned} \quad (8)$$

where $S_{\delta-1} = 2\pi^{\delta/2}/\Gamma(\delta/2)$ denotes the surface of a unit radius sphere in δ dimensions while M_D is related to the D dimensional reduced Planck constant \overline{M}_D by $M_D = (2\pi)^{\delta/(2+\delta)}\overline{M}_D$.

Table 1. 95% CL limits from Tevatron/LEP [11]

δ	2	3	4	5	6
M_D (TeV)	1.45	1.09	0.87	0.72	0.65

2 Detecting the Higgs at the LHC and LC

Fig. 1 shows that the branching ratio of the Higgs into invisible states can be substantial for M_D values in the TeV range both when $m_h = 120$ GeV (upper part), therefore below the WW threshold, and when $m_h = 237$ GeV (lower part), a value greater than the WW threshold and corresponding to the 95% CL limit from LEP data with $m_t = 178$ GeV. As a consequence this invisible width causes a significant suppression of the LHC Higgs rate in the standard visible channels and for any given value of the Higgs boson mass, there is a considerable parameter space region where the invisible decay width of the Higgs boson could be the Higgs discovery channel. This is exemplified in Figure 2 for $m_h = 120$ GeV and $m_h = 237$ GeV, $\delta = 2, 3$. In the green (light grey) region the Higgs signal in standard channels drops below the 5σ threshold with 100 fb^{-1} of LHC data. But in the area above the bold blue line the LHC search for invisible decays in the fusion channel yields a signal with an estimated significance exceeding 5σ . We have here rescaled to higher luminosity the statistical significance of the analysis presented in [12]. The solid vertical line at the largest M_D value in each figure shows the upper limit on M_D which can be probed at the 5σ level by the analysis of jets/ γ with missing energy at the LHC [13]. The middle dotted vertical line shows the value of M_D below which the theoretical computation at the LHC is ambiguous — a signal could still be present there, but its magnitude is uncertain [14]. The dashed vertical line at the lowest M_D value is the 95% CL lower limit coming from combining Tevatron and LEP/LEP2 limits (from Table 1). The regions above the yellow (light grey) line are the parts of the parameter space where the LC invisible Higgs signal will exceed 5σ . We have employed the $\sqrt{s} = 350$ GeV, $L = 500\text{ fb}^{-1}$ results of [15] looking for a peak in the M_X mass spectrum in $e^+e^- \rightarrow ZX$ events.

In conclusion, whenever the Higgs boson sensitivity is lost due to the suppression of the canonical decay modes, the invisible rate is large enough to still ensure detection through the WW fusion channel.

The parameters of the model can be determined by combining several measurements that can be performed at LHC and a LC: here we closely follow the discussion of [10].

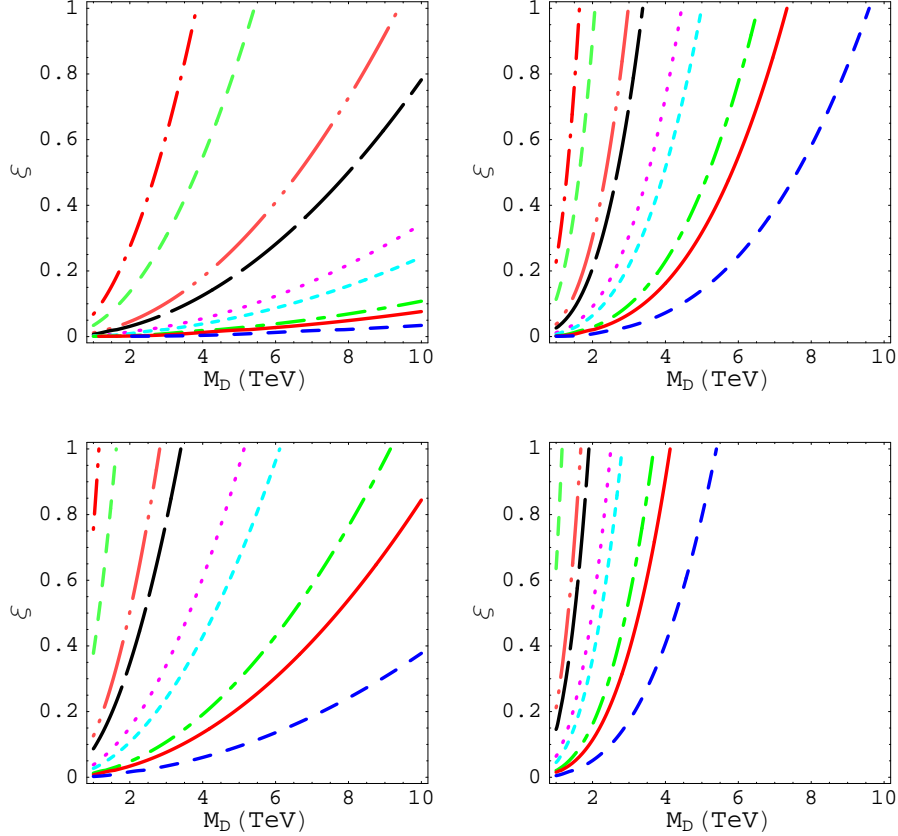


Fig. 1. Contours of fixed $BR(h \rightarrow inv)$ in the $M_D(\text{TeV}) - \xi$ parameter space for $\delta = 2$ (left) and $\delta = 4$ (right) in the upper part for $m_h = 120$ GeV and in the lower part for $m_h = 237$ GeV. In order of increasing ξ values, the contours correspond to: 0.0001 (large blue dashes), 0.0005 (solid red line), 0.001 (green long dash – short dash line), 0.005 (short cyan dashes), 0.01 (purple dots), 0.05 (long black dashes), 0.1 (chartreuse long dashes with double dots), 0.5 (green dashes), and 0.85 (red long dash, short dot line at high ξ and low M_D)

For the LHC Higgs signal in visible channels, we compute the $\Delta\chi^2$ for a model relative to expectations for an input model as follows.

For some central choice of parameters, define $S_0 = f_0 B_0$ and $N_{SD0} = S_0/\sqrt{B_0}$. Then, $\Delta S_0^2 = S_0 + B_0 = B(1 + f_0) = [S_0/N_{SD0}]^2(1 + f_0)$. As a result, we can

compute $\Delta\chi^2$ for some other choice of parameters that yields signal rate S as

$$\Delta\chi^2 = \frac{(S - S_0)^2}{\Delta S_0^2} = \frac{N_{SD0}^2}{1 + f_0} \left[\frac{S}{S_0} - 1 \right]^2 = \frac{N_{SD0}^2}{1 + f_0} \left[\left(\frac{1 - BR_{h_{eff} \rightarrow invisible}}{1 - BR_{h_{eff} \rightarrow invisible}^0} \right) - 1 \right]^2. \quad (9)$$

We obtain N_{SD0} as previously described. In principle, f_0 should be computed on a channel by channel basis. In [10] we have adopted an average value of $S_{SM}/B = f_{SM}$ for the SM Higgs rates (assuming no invisible decays) that applies to all channels and compute $f_0 = (1 - BR_{h_{eff} \rightarrow invisible}^0) f_{SM}$. We have chosen $f_{SM} = 0.5$, a value that we consider somewhat conservative except for the $\gamma\gamma$ final state mode.

For the LHC Higgs signal in the invisible final state, we employed the detailed results of [16] (used in [12]), in which the Higgs signal and background event rates are given for the $WW \rightarrow Higgs \rightarrow invisible$ channel assuming SM production rate and 100% invisible branching ratio. The background cross section extracted from [16] is $\sigma_{B_{inv}} = 409.6$ fb. Signal cross sections, $\sigma_{S_{inv}^{SM}}$, for 100% invisible branching ratio are given for Higgs masses ranging from 110 GeV to 400 GeV. These cross sections are multiplied by the assumed integrated luminosity to obtain the signal and background rates, S_{inv}^{SM} and B_{inv} . We rescale the signal rate using $S_{inv}^{h_{eff}} = BR_{h_{eff} \rightarrow invisible} S_{inv}^{SM}$ and compute the error in the signal rate as $[\Delta S_{inv}^{h_{eff}}]^2 = S_{inv}^{h_{eff}} + B_{inv}$.

As we shall see, a TeV-class e^+e^- linear collider will be able to improve the determination of the ADD model parameters very considerably with respect to the LHC alone, making use of the Higgs signals in both visible and invisible final states and also of the $\gamma + E_T$ signal. For the $\gamma + E_T$ signal, we have employed the TESLA study results of [17] for the signal. The signal cross section in Fig. 1 of [17] was computed assuming 80% e^- beam polarization and 60% e^+ beam polarization, as well as cuts on the final state photon of $E_\gamma < 0.625E_{beam}$, $|\cos\theta_\gamma| < 0.90$ and $E_T > 0.06E_{beam}$. The $e^+e^- \rightarrow \nu_e\bar{\nu}_e + \gamma$ background has been computed using the KK [18] and **nunugpv** [19] simulation programs. Results from the two programs agree well. For the polarization choices and cuts listed above, we find $\sigma_B = 102(106.7), 125.7$ (123.7), and 202.3(195.6) fb using the KK (**nunugpv**) programs at $\sqrt{s} = 1000, 800, 500$ GeV, respectively. (The $\sqrt{s} = 800$ GeV result is in rough agreement with that employed in [17].)

Figure 3 considers fixed input parameters of $\delta = 2$ and $\xi = 0.5$; the input M_D is varied between the first three subfigures while the luminosities assumed are reduced for the fourth figure. We observe that the ability of the LHC to determine the input parameters is very limited; however by including the precision LC data, quite precise δ and M_D determination is possible so long as M_D is not too big. In contrast, the precision of the ξ determination leaves much to be desired in all but the first ($M_D = 2$ TeV) case where the invisible branching ratio is large and the SM visible modes are suppressed and varying rapidly as a function of ξ . Comparing the lower right figure to the upper right figure, we see that the decline in precision

resulting from lowering the LHC and LC luminosities is not that drastic.

I would like to thank M. Battaglia and J. Gunion for their collaboration on the topics discussed in this talk.

References

- [1] G. Belanger, F. Boudjema, A. Cottrant, R. M. Godbole, and A. Semenov. The MSSM invisible Higgs in the light of dark matter and g- 2. *Phys. Lett.*, B519:93–102, 2001.
- [2] Stephen P. Martin and James D. Wells. Motivation and detectability of an invisibly-decaying Higgs boson at the Fermilab Tevatron. *Phys. Rev.*, D60:035006, 1999.
- [3] Anjan S. Joshipura and J. W. F. Valle. Invisible Higgs decays and neutrino physics. *Nucl. Phys.*, B397:105–122, 1993.
- [4] K. Belotsky, D. Fargion, M. Khlopov, R. Konoplich, and K. Shibaev. Invisible Higgs boson decay into massive neutrinos of 4th generation. *Phys. Rev.*, D68:054027, 2003.
- [5] N. Arkani-Hamed, S. Dimopoulos, and G. R. Dvali. *Phys. Lett.*, B429:263–272, 1998.
- [6] I. Antoniadis, N. Arkani-Hamed, S. Dimopoulos, and G. R. Dvali. *Phys. Lett.*, B436:257–263, 1998.
- [7] G. F. Giudice, R. Rattazzi, and J. D. Wells. *Nucl. Phys.*, B595:250–276, 2001.
- [8] J. D. Wells. hep-ph/0205328.
- [9] M. Battaglia et al in B. C. Allanach et al., Les Houches 'Physics at TeV colliders 2003' Beyond the Standard Model working group: Summary report. 2004.
- [10] M. Battaglia, D. Dominici, and J. F. Gunion. In preparation.
- [11] Gian Francesco Giudice and Alessandro Strumia. Constraints on extra-dimensional theories from virtual- graviton exchange. *Nucl. Phys.*, B663:377–393, 2003.
- [12] S. Abdullin *et al.* CMS NOTE-2003/033.
- [13] L. Vacavant and I. Hinchliffe. *J. Phys.*, G27:1839–1850, 2001.
- [14] G. F. Giudice, R. Rattazzi, and J. D. Wells. *Nucl. Phys.*, B544:3–38, 1999.
- [15] M Schumacher. Note. LC-PHSM 2003-096.
- [16] Oscar J. P. Eboli and D. Zeppenfeld. Observing an invisible Higgs boson. *Phys. Lett.*, B495:147–154, 2000.
- [17] Graham W. Wilson. LC-PHSM-2001-010, Feb. 2001.
- [18] B. F. L. Ward, S. Jadach, and Z. Was. Precision calculation for $e^+e^- \rightarrow 2f$: The k mc project. *Nucl. Phys. Proc. Suppl.*, 116:73–77, 2003.
- [19] G. Montagna, O. Nicrosini, and F. Piccinini. Nunugpv: A Monte Carlo event generator for $e^+e^- \rightarrow \nu\bar{\nu}\gamma$ events at lep. *Comput. Phys. Commun.*, 98:206, 1996.

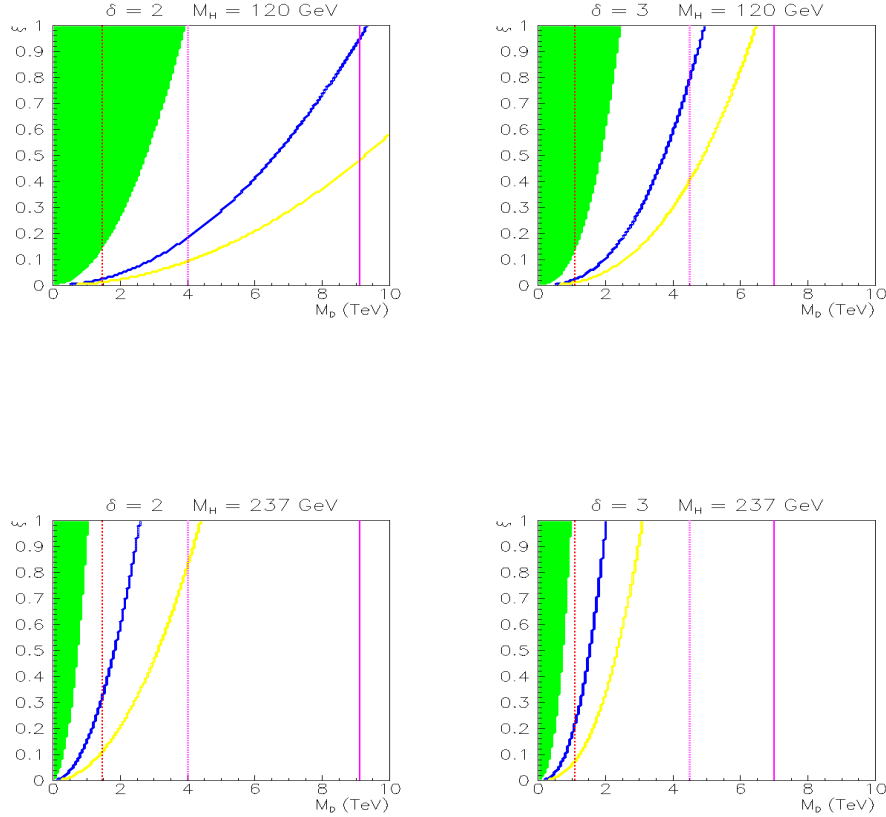


Fig. 2. Invisible decay width effects in the ξ - M_D plane for $m_h = 120$ GeV (upper) and $m_h = 237$ GeV (lower). The plots are for $\delta = 2$ (left) and $\delta = 3$ (right). The green (grey) regions indicate where the Higgs signal at the LHC drops below the 5σ threshold for 100 fb^{-1} of data. The regions above the blue (bold) line are the parts of the parameter space where the LHC invisible Higgs signal in the WW -fusion channel exceeds 5σ significance. The solid vertical line at the largest M_D value in each figure shows the upper limit on M_D which can be probed at the 5σ level by the analysis of jets/ γ with missing energy at the LHC. The middle dotted vertical line shows the value of M_D below which the theoretical computation at the LHC is ambiguous — a signal could still be present there, but its magnitude is uncertain. The dashed vertical line at the lowest M_D value is the 95% CL lower limit coming from combining Tevatron and LEP/LEP2 limits. The regions above the yellow (light grey) line are the parts of the parameter space where the LC invisible Higgs signal will exceed 5σ assuming $\sqrt{s} = 350$ GeV and $L = 500 \text{ fb}^{-1}$.

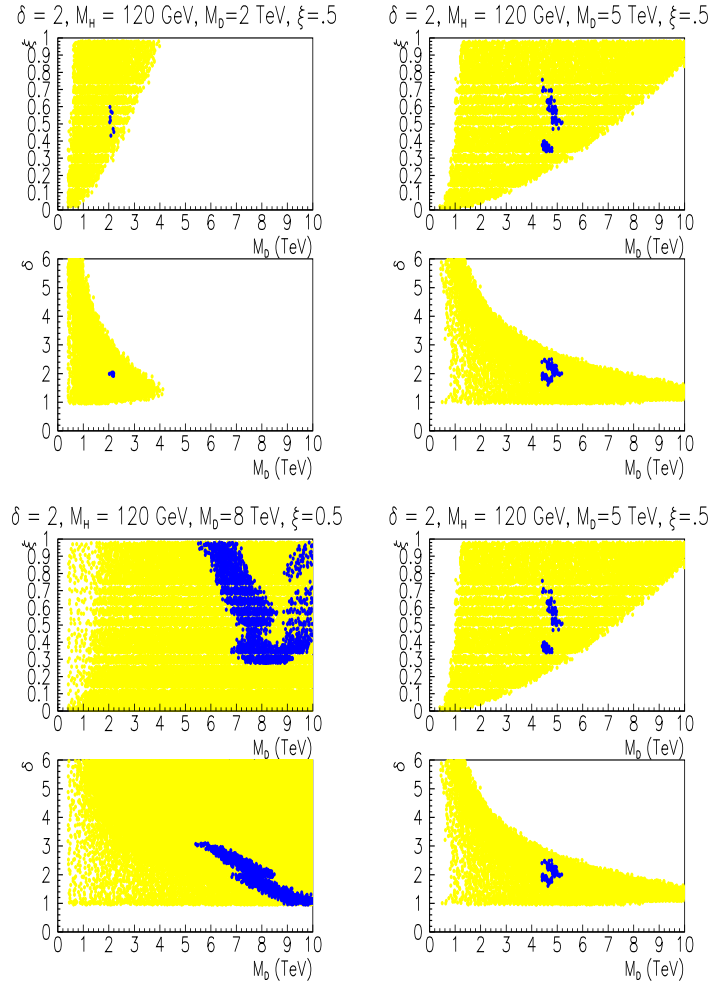


Fig. 3. 95% CL contours for determination of the ADD parameters, M_D , ξ and δ assuming $m_{h_{eff}} = 120$ GeV. The plots are all for $\delta = 2$ and $\xi = 0.5$. The upper two plots and lower left plot are obtained assuming $L = 100 \text{ fb}^{-1}$ at the LHC, $\sqrt{s} = 350$ GeV Higgs measurements at the LC, and $\sqrt{s} = 500$ GeV and $\sqrt{s} = 1000$ GeV $\gamma + E_T$ measurements at the LC with $L = 1000 \text{ fb}^{-1}$ and $L = 2000 \text{ fb}^{-1}$ at the two respective energies. They are for different M_D^0 values: upper left — $M_D^0 = 2 \text{ TeV}$; upper right — $M_D^0 = 5 \text{ TeV}$; lower left — $M_D^0 = 8 \text{ TeV}$. The lower right plot is a repeat of the $M_D^0 = 5 \text{ TeV}$ case, but assuming lower integrated luminosities: $L = 30 \text{ fb}^{-1}$ at the LHC and $L = 500 \text{ fb}^{-1}$ and $L = 1000 \text{ fb}^{-1}$ at $\sqrt{s} = 500$ GeV and $\sqrt{s} = 1000$ GeV at the LC. The larger light grey (yellow) regions are the 95% CL regions in the ξ, M_D and δ, M_D planes using only $\Delta\chi^2(LHC)$. The smaller dark grey (blue) regions or points are the 95% CL regions in the ξ, M_D and δ, M_D planes using $\Delta\chi^2(LHC + LC)$.